AD-A286 081

ARMY RESEARCH LABORATORY
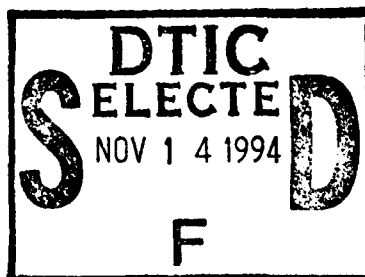
The Calculation and Measurement of Helmholtz Coil Fields

by David J. DeTroye and
Ronald J. Chase

ARL-TN-35

DTIC
SELECTED
NOV 1 4 1994
F

November 1994

94-34824

424778

DTIC QUALITY INSPECTED 5

94 11 0 026

REPORT DOCUMENTATION PAGE

Public reporting burden for this collection of information is estimated to average 1 hour per response, including the time for reviewing instructions, searching existing data sources, gathering and maintaining the data needed, and completing and reviewing the collection of information. Send comments regarding this burden estimate or any other aspect of this collection of information, including suggestions for reducing this burden, to Washington Headquarters Services, Directorate for Information Operations and Reports, 1215 Jefferson Davis Highway, Suite 1204, Arlington, VA 22202-4302, and to the Office of Management and Budget, Paperwork Reduction Project (0704-0188), Washington, DC 20503

1 AGENCY USE ONLY (Leave blank)	2. REPORT DATE	3 REPORT TYPE AND DATES COVERED
	November 1994	Final, October 1993–October 1994

4 TITLE AND SUBTITLE	5 FUNDING NUMBERS
The Calculation and Measurement of Helmholtz Coil Fields	PE 62120

6 AUTHOR(S)

David J. DeTroye and Ronald J. Chase

7 PERFORMING ORGANIZATION NAME(S) AND ADDRESS(ES)	8 PERFORMING ORGANIZATION REPORT NUMBER
U.S. Army Research Laboratory Attn AMSRL-WT-NF 2800 Powder Mill Road Adelphi, MD 20783-1197	ARL-TN-35

9 SPONSORING/MONITORING AGENCY NAME(S) AND ADDRESS(ES)	10 SPONSORING/MONITORING AGENCY REPORT NUMBER
U.S. Army Materiel Command 5001 Eisenhower Avenue Alexandria, VA 22333-0001	

11 SUPPLEMENTARY NOTES

AMS code 612120 H250011
ARL PR 3FE7E5

12a DISTRIBUTION/AVAILABILITY STATEMENT	12b DISTRIBUTION CODE
Approved for public release; distribution unlimited.	

13 ABSTRACT (Maximum 200 words)

Helmholtz coils are used to develop uniform magnetic fields for a variety of research applications. Helmholtz coils can be easily constructed, and the fields easily calculated. This makes them especially useful in calibrating sensors and numerous other low frequency magnetic field testing applications. This particular report will discuss the calculation and measurement of Helmholtz coil fields to be used for testing of composite materials to low frequency magnetic fields.

14 SUBJECT TERMS		15. NUMBER OF PAGES
Testing, Helmholtz coils, composite, magnetic field		21
		16. PRICE CODE

17 SECURITY CLASSIFICATION OF REPORT	18. SECURITY CLASSIFICATION OF THIS PAGE	19. SECURITY CLASSIFICATION OF ABSTRACT	20. LIMITATION OF ABSTRACT
Unclassified	Unclassified	Unclassified	UL

NSN 7540-01-280-5500

1

Contents

Appendix

Figures

Table

1. Background

Composite materials are being increasingly used throughout the Army as a means of decreasing the weight and increasing the strength of Army systems. With the increased use of composite materials, the question of electromagnetic shielding must be answered. The Army Research Laboratory (ARL) is currently involved in a composite shielding program whose objective is to examine the composites used in Army systems and characterize them electromagnetically. The approach used has been to develop a composite characterization laboratory that will measure the electrical properties of composites. The Helmholtz coil is one tool that will be used in the characterization laboratory.

2. Introduction

Helmholtz coils are used to develop uniform magnetic fields for a variety of research applications. Helmholtz coils can be easily constructed and the fields easily calculated. This makes them especially useful in calibrating sensors and numerous other low-frequency magnetic-field testing applications. This report discusses the calculation and measurement of Helmholtz coil fields to be used for testing of composite materials to low-frequency magnetic fields. Future composite testing of this nature will be based on American National Standard ANSI/ASTM A698-74, "Standard Test Method for Magnetic Shield Efficiency in Attenuating Alternating Magnetic Fields."

3. Test Configuration

The Helmholtz coils were constructed in accordance with the guidelines in the ASTM 698-74 standard. They were fabricated from ¾-in. plywood, ½-in. Extren® threaded rod, and 14 AWG copper (coated) wire. Each coil had a diameter of approximately 47.5 in. (1.219 m), with 48 turns each of the copper wire. The coils are shown in figure 1. Sixteen ½-in. Extren threaded rods were used to form the circular shape of the coil. The magnetic fields associated with the Helmholtz coils were measured with two single-turn shielded loops. Both were constructed from 0.141-in. copper jacketed cable, one with a diameter of 2 in. and the other of 3 in. Additional information on the calibration of the loops is provided in section 4.

A Hewlett Packard (HP) 3577A network analyzer was used to measure the magnetic fields of the Helmholtz coil. The output of the analyzer was connected to an audio amplifier, whicn was connected to

the Helmholtz coil. The reference channel monitored the current in the loop. Channel A recorded the voltage associated with the 2- or 3-in. loops placed inside the coil. The complete test configuration is shown in figure 2.
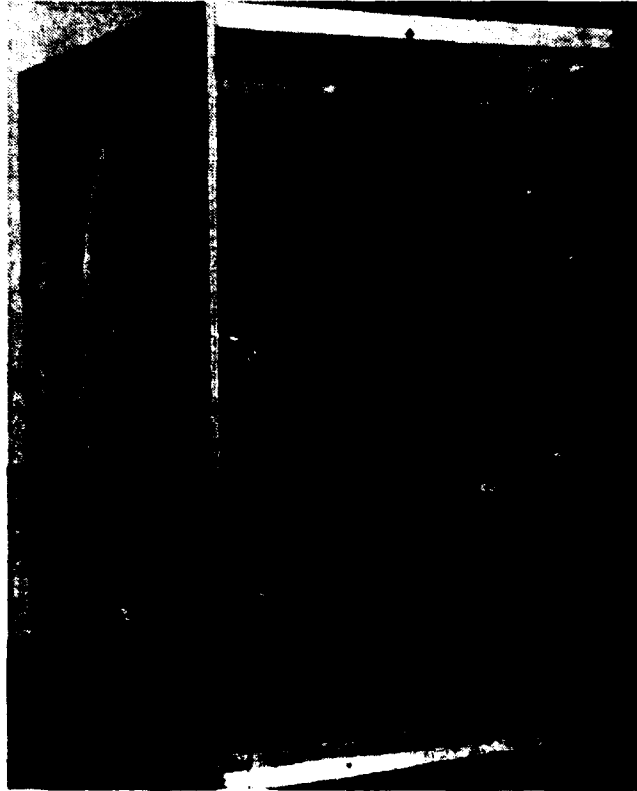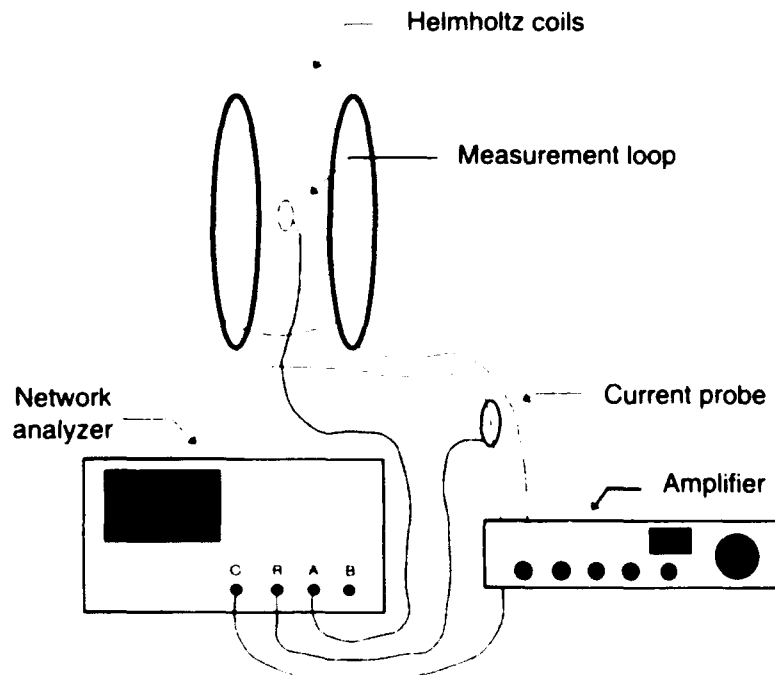
Figure 1. Helmholtz coil construction.

Figure 2. Test configuration.

4. Measurement Loop Calibration

Two electrostatically shielded single-turn loops (one 2-in., one 3-in.) were used to measure the fields associated with the Helmholtz coils. Both were constructed as shown in figure 3. The open-circuit voltage at the loop output terminals can easily be calculated by

$$V_{oc} = 2\pi f NAB \ , \tag{1}$$

where

V_{oc} = open-circuit voltage at loop's output terminals,
f = frequency (in hertz),
N = number of turns in loop (one turn),
A = area of loop (in meters), and
B = magnetic flux density (in teslas).

The loops were calibrated in a transverse electromagnetic (TEM) cell known as a Crawford cell. Using an HP 3577A network analyzer, we measured the loop voltage as a function of output voltage applied to the TEM cell versus frequency. Knowing the physical dimensions of the TEM cell and the measured area of the loops, we could determine the ratio of the measured versus reference voltages; to determine the calculated response, we applied this ratio to

$$R_C = 20 \log(V_{oc}/V_{ref}) \ , \tag{2}$$

Figure 3. Measurement loop construction.
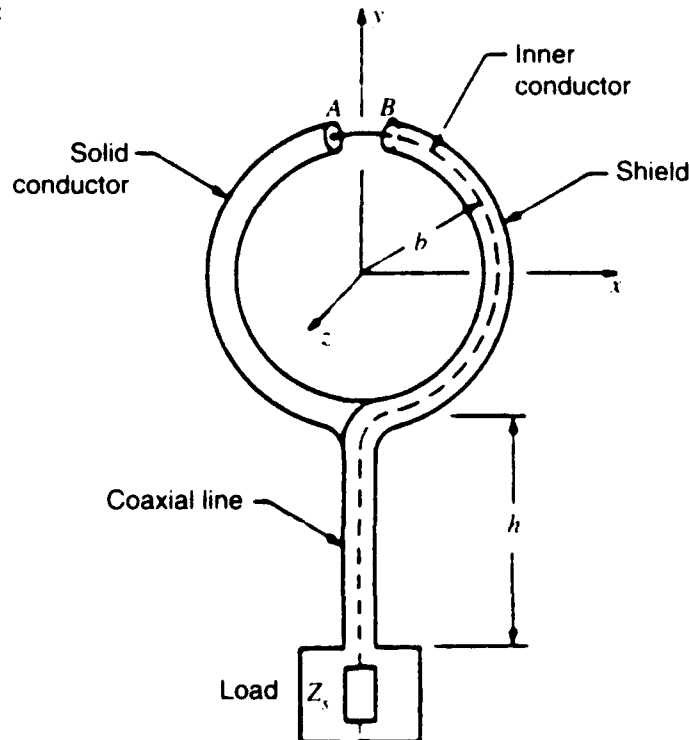
where

R_C = calibrated response,
V_{oc} = open-circuit voltage at loop's output terminals, and
V_{ref} = reference voltage applied to the TEM cell.

The measured and calculated results are shown in table 1 for 100 kHz. Figure 4 compares the measured and calculated responses for a frequency range of 100 kHz to 10 MHz for both the 2- and 3-in. loops. One can see that the calculated and measured responses follow each other to well within 0.5 dB. Based on equation (1), it is assumed that both of the loops would continue to fall at 20 dB per decade to dc. Because of limitations in the measurement system, the loops could not be calibrated below 100 kHz.

5. Helmholtz Coil Predicted Results

The magnetic fields generated by a circular wire loop can be derived according to the following procedure. The electromagnetic (EM) fields generated by a circular wire loop carrying current I will satisfy the Maxwell equations. For a wire loop (or a coil) excited with low-frequency current, almost all the energy is stored in the magnetic field. This energy is determined from the concepts and rules of circuit theory. Circuit theory can be regarded as describing a special class of solutions of the Maxwell equations that result from using the

Table 1. Loop calibration results.

Loop dimension (in.)	Measured area (m)	Calculated response (dB)	TEM cell measured response (dB)	Difference (dB)
2	2.545	-95.1511	-94.9368	0.2143
3	5.572	-88.3447	-87.8906	0.4541

(a)

(b)
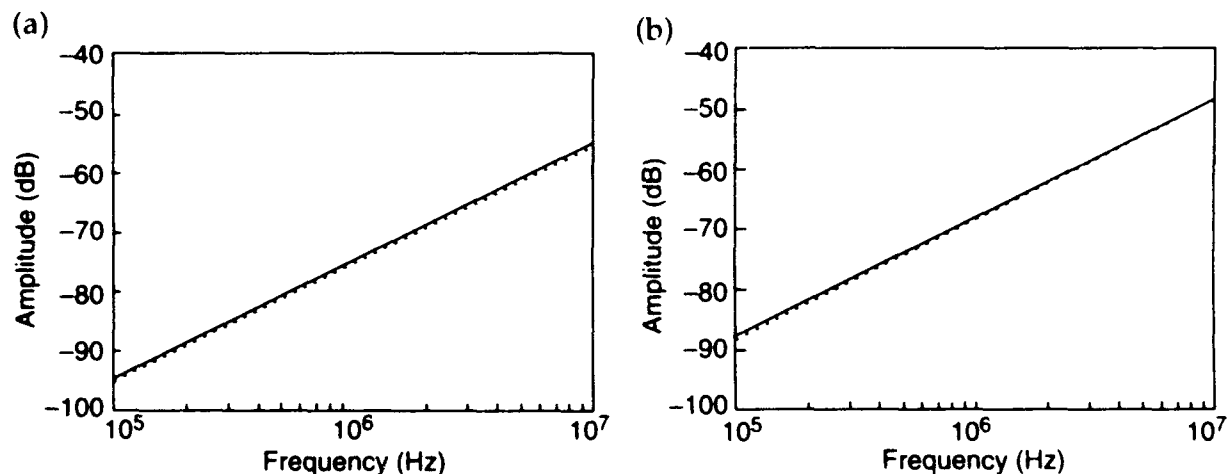
Figure 4. Measured (solid) and calculated (dotted) responses of (a) 2- and (b) 3-in. loops.

8

first term of a power series solution for the fields. The fields computed with this approximation are called quasi-static. EM phenomena such as radiation are neglected in the quasi-static approximation.[1]

A general rule of thumb for circuit elements excited by sinusoidal voltage or current is that the quasi-static approximation will be extremely good when the physical size of the element is sufficiently small with respect to the wavelength of the source excitation. This restriction will be satisfied if the phase of the voltage (current) is approximately the same over the spatial extent of the element. For a circular loop, this condition requires that the current be nearly constant over the circumference of the loop. The current can change in time, but at each instant of time, the current in every part of the loop should have the same value. Therefore, the quasi-static approximation will be very good as long as $2\pi a \ll \lambda$ (or in terms of frequency instead of wavelength, $v \ll c/10a$), where a is the loop radius and c is the velocity of light in free space.

One can find the EM fields generated by a loop in this order of approximation by determining the current in the loop employing circuit theory and using that uniform current as the source of the vector potential from which the fields can easily be derived. This is the approach followed below.[2]

Figure 5 shows the coordinates and variables for a loop of radius a located in the xy plane. The loop is assumed to have a total current I. The vector potential for a general current distribution can then be written as

$$\vec{A}(\vec{r}) = \frac{\mu_0}{4\pi} \int \frac{I \, \vec{dl}}{|\vec{r} - \vec{r}'|} \ .$$

where A is the vector potential and I is the current in the loop. From the direction of the current, A has only a ϕ component, and by symmetry A is independent of the variable ϕ. In setting up the integration, we arbitrarily set $\phi = 0$ to simplify the results. With the symbols given in figure 5, the following can be derived:

$$\vec{dl} = (-a \sin \phi', \ a \cos \phi', \ 0) d\phi' \ ,$$
$$\vec{r} = (r \sin \theta, \ 0, \ r \cos \theta) \ ,$$
$$\vec{r}' = (a \cos \phi', \ a \sin \phi', \ 0) \ ,$$
$$|\vec{r} - \vec{r}'| = \sqrt{r^2 + a^2 - 2ra \sin \theta \cos \phi'} \ .$$

[1] R. M. Fano, L. J. Chu, and R. B. Adler, *Electromagnetic Fields, Energy, and Forces,* John Wiley & Sons, Inc. (1960).
[2] William R. Smythe, *Static and Dynamic Electricity,* Hemisphere Publishing Corp. (1989).

Figure 5. Coordinates
and variables
describing a circular
loop used to express
EM fields.
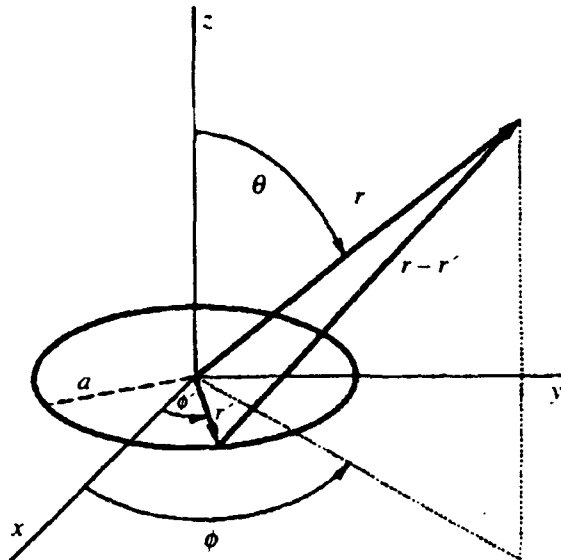
Substituting these variables in the integral, we note that the integral involving sin ϕ' vanishes (it is odd), as it should since only an A_ϕ component must survive, and the integral involving cos ϕ' (even) allows the range of integration to be halved. This results in

$$A_\phi(r,\theta) = \frac{\mu_0 Ia}{2\pi} \int_0^\pi \frac{\cos \phi' \, d\phi'}{\sqrt{r^2 + a^2 - 2ra \sin \theta \cos \phi'}} \ .$$

It is more convenient to express this integral in terms of cylindrical coordinates using $r^2 = \rho^2 + z^2$ and $\sin \theta = \rho/\sqrt{\rho^2 + z^2}$, which gives

$$A_\phi(\rho,z) = \frac{\mu_0 IA}{2\pi} \int_0^\pi \frac{\cos \phi' \, d\phi'}{\sqrt{\rho^2 + z^2 + a^2 - 2a\rho \cos \phi'}} \ .$$

This integral does not have a closed form; however, there is a transformation that results in tabulated functions. Change the variable to make the upper limit of the integral $\pi/2$, by using $\phi' = \pi + 2\phi$. The integral becomes

$$A_\phi(\rho,z) = \frac{\mu_0 Ia}{\pi} \int_0^{\frac{\pi}{2}} \frac{(2 \sin^2 \phi - 1) \, d\phi}{\sqrt{(a + \rho)^2 + z^2 - 4a\rho \sin^2 \phi}} \ .$$

If we define $k^2 = \dfrac{4a\rho}{(a + \rho)^2 + z^2}$, the integral is transformed into

$$A_\phi(\rho,\phi) = \frac{\mu_0 I}{\pi k} \sqrt{\frac{a}{\rho}} \left[\left(1 - \tfrac{1}{2} k^2\right) K(k) - E(k) \right] \ ,$$

with

$$K(k) = \int_0^{\frac{\pi}{2}} \frac{d\phi}{\sqrt{1 - k^2 \sin^2 \phi}} \quad \text{and} \quad E(k) = \int_0^{\frac{\pi}{2}} \sqrt{1 - k^2 \sin^2 \phi} \; d\phi \; .$$

K is the complete elliptic integral of the first kind, and E is the complete elliptic integral of the second kind. Both are tabulated functions.

The magnetic fields are computed from the vector potential by $\vec{B} = \nabla \times \vec{A}$, giving two components:

$$B_\rho(\rho,z) = -\frac{\partial A_\phi}{\partial z} \quad \text{and} \quad B_z(\rho,z) = \frac{1}{\rho} \frac{\partial}{\partial \rho} (\rho A_\phi) \; .$$

To calculate these derivatives, we will need the derivatives of K, E, and k, since they are functions of ρ and z. The math is straightfoward and the results are summarized below:

$$\frac{\partial K}{\partial k} = \frac{E}{k(1 - k^2)} - \frac{K}{k} \quad \text{and} \quad \frac{\partial E}{\partial k} = \frac{E}{k} - \frac{K}{k} \; ,$$

$$\frac{\partial k}{\partial \rho} = \frac{k}{2\rho} - \frac{k^3}{4\rho} - \frac{k^3}{4a} \quad \text{and} \quad \frac{\partial k}{\partial z} = -\frac{zk^3}{4a\rho} \; .$$

The final expression for the magnetic field components becomes

$$B_\rho(\rho,z) = \frac{\mu_0 I}{2\pi} \frac{z}{\rho\sqrt{(\rho + a)^2 + z^2}} \left[\frac{a^2 + \rho^2 + z^2}{(a - \rho)^2 + z^2} E(k) - K(k) \right] \; ,$$

$$B_z(\rho,z) = \frac{\mu_0 I}{2\pi} \frac{1}{\sqrt{(\rho + a)^2 + z^2}} \left[\frac{a^2 - \rho^2 - z^2}{(a - \rho)^2 + z^2} E(k) - K(k) \right] \; .$$

For a single loop in the xy plane, we can find the magnetic field components at any location ρ and z by first determining k from the above definition, and then substituting into the above formulas.

We can check the accuracy of these expressions for the simple case of the magnetic field components along the axis of a loop. On the axis, $\rho = 0$, which implies $k = 0$, and hence $K(0) = E(0) = \pi/2$. The expression for B_ρ becomes indeterminate, but application of l'Hopital's rule gives $B_\rho = 0$. The expression for B_z becomes $0.5\mu_0 a^2 I / \sqrt{(a^2 + z^2)^3}$, as expected.

Calculating the magnetic fields from a Helmholtz coil requires fields computed for two loops having the same axis, located in the planes

at $z = -d$ and $z = +d$. The separation distance $2d$ is related to the loop radius by $d = a/2$. The expression for the total magnetic field written in terms of the above derivation is just the sum of the individual fields from each loop. Using the notation and results derived earlier for an individual loop, one can write

$$B_\rho^{total}(\rho,z) = B_\rho(\rho,z+d) + B_\rho(\rho,z-d) \, ,$$
$$B_z^{total}(\rho,z) = B_z(\rho,z+d) + B_z(\rho,z-d) \, .$$

Once the solutions were obtained, the variables were substituted for the actual Helmholtz coil. The diameter of the coil was measured at 1.219 m, the average current measured (see sect. 6) was 0.019052 A, and the number of turns was 48.

6. Measured Results

Numerous magnetic field measurements were taken on the test configuration described in section 3. The objective of the magnetic field measurements was to verify the predicted response and determine the size of the test volume. This was done by essentially mapping the inside of the Helmholtz coil. A cylindrical coordinate system was used for consistency with the predicted results. Both the ρ and z coordinates were varied in 2-in. increments. Because of symmetry, the ϕ component was not recorded, and only one quadrant was measured.

Figure 6 is a measurement of the Helmholtz coil's fields as a function of frequency. Figure 6 clearly shows that the coil has a resonance at approximately 58 kHz, which would mean that the usable frequency range of the Helmholtz coil is between dc and 40 kHz. Frequencies above 40 kHz should not be used.

The measured results compared very well to the calculated results, as is shown in figures 7 to 9. Figure 7 shows a three-dimensional comparison between the measured and calculated z-component of the magnetic field as a function of ρ and z. One can see that the two compare very well in wave shape and magnitude. Figure 8 shows a two-dimensional comparison of the measured versus calculated magnetic field as a function of z on the centerline ($\rho = 0$).

The peak magnitude of the measured field is 1.345×10^{-6} T (teslas), while the calculated is 1.348×10^{-6} T. Both are essentially the same magnitude. The measured data have a noticeable peak at $z = 0$, where the calculated data are flat out to $z = \pm 0.1$. This difference (0.37 percent) cannot be fully explained, but one possibility is that the measurement loop was not perpendicular to the incident mag-

Figure 6. Measured resonance of Helmholtz coil.
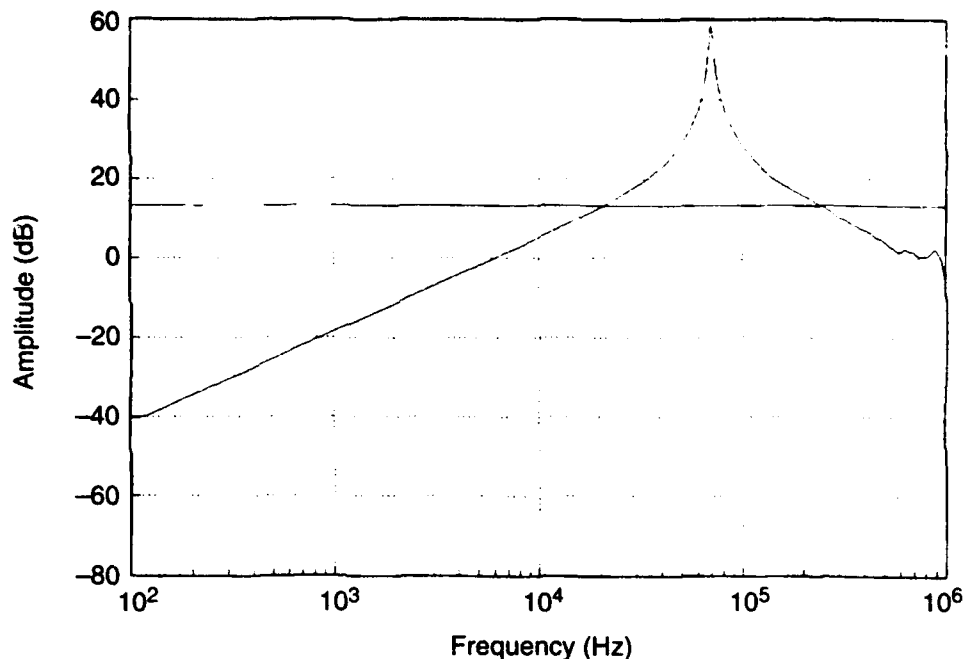
netic field. Equation (1) assumes that the magnetic field is normal to the plane of the measurement loop. When the measurement loop is not normal to the incident field, equation (1) has to be multiplied by the sine of the angle between the plane of the loop and the incident field. A *difference of 0.37 percent is equivalent to the 2-in. loop being* off less than 5° or ³⁄₃₂ in. above and below the normal plane. While great care was taken to map the fields inside the coils, the measurement loops were only sighted in for being perpendicular, and errors of this magnitude were possible. Figure 9 is another representation of the same data, shown as contour plots. The contour plots show that the field is uniform at 1.3×10^{-6} T for most of the inner region. Again, one can see that the measured data compare very well with the calculated.

13

Figure 7. Three-dimensional plots of magnitude of magnetic field $B(z)$ versus B and ρ: (a) measured and (b) calculated.

(a)

(b)
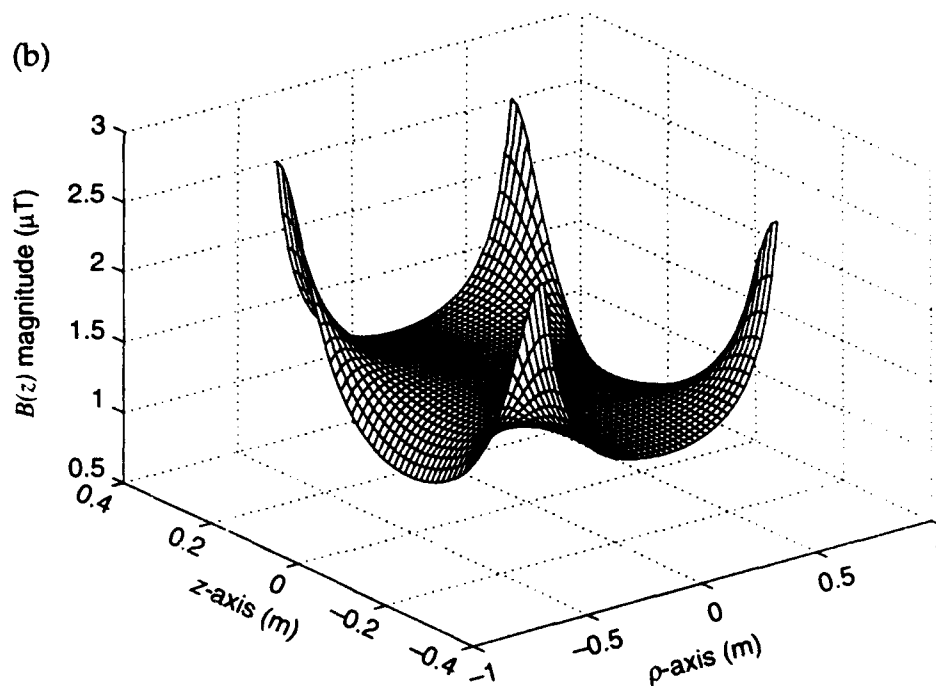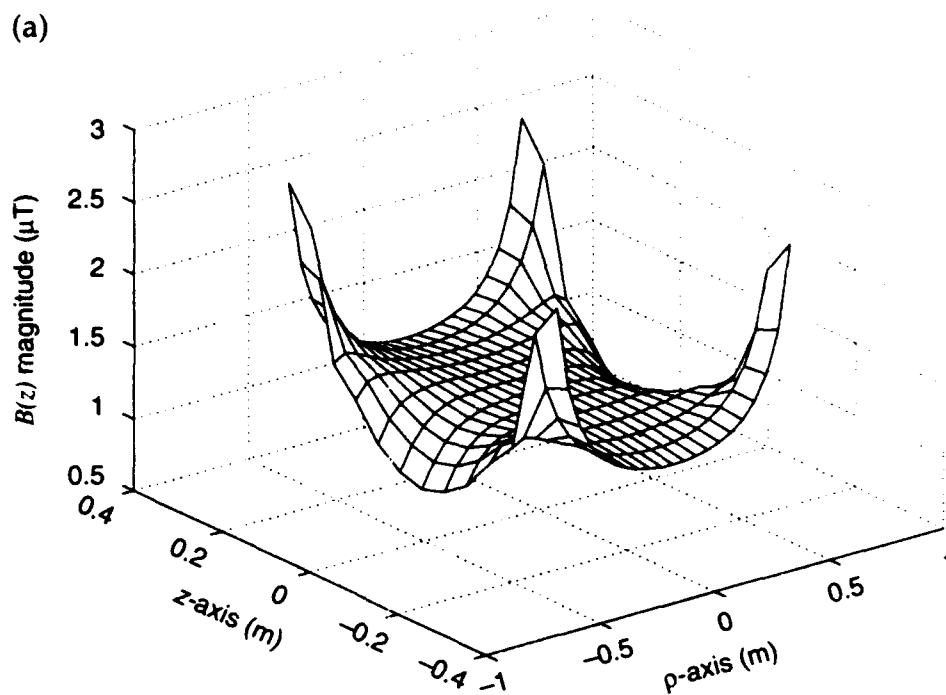
Figure 8. Magnetic field *B(z)* on centerline as a function of *z*: (a) measured and (b) calculated.
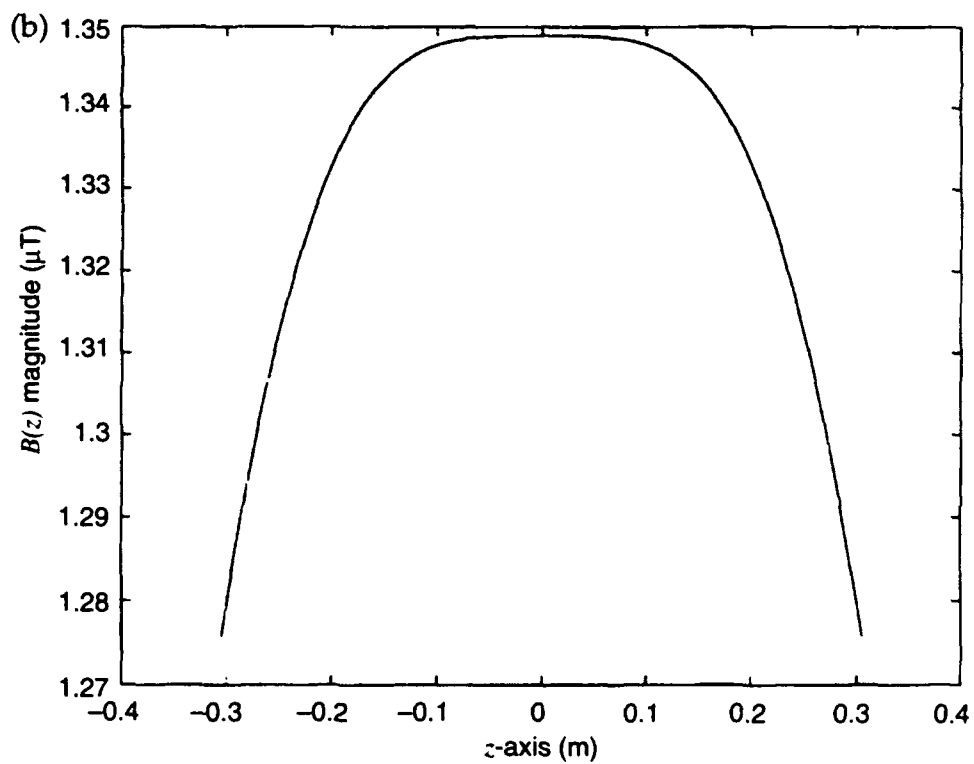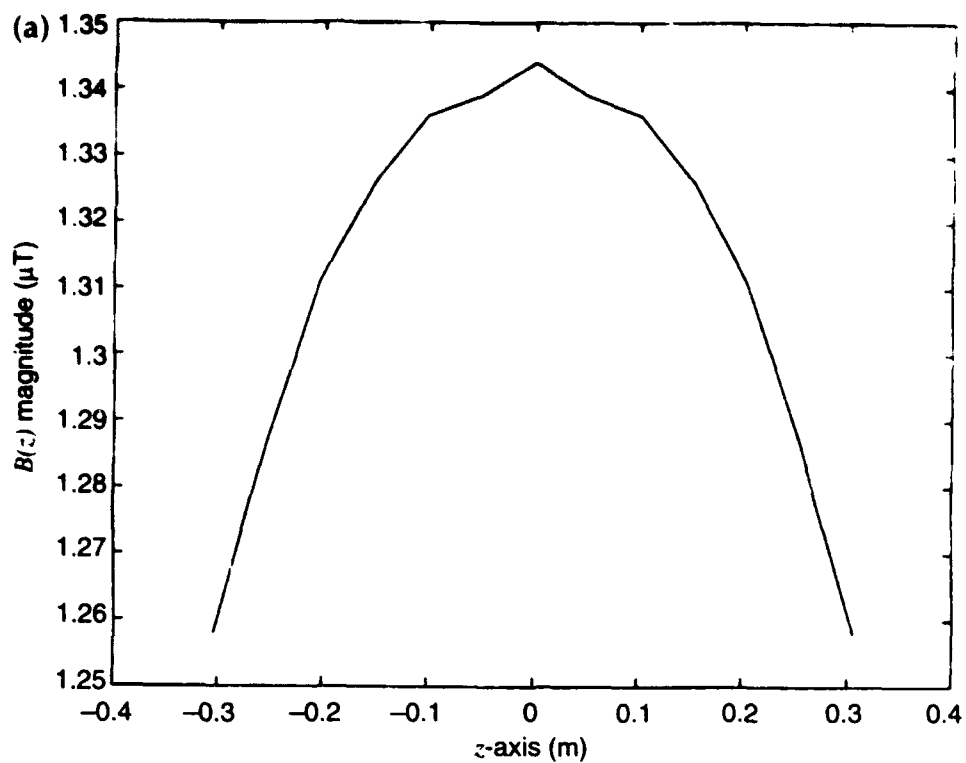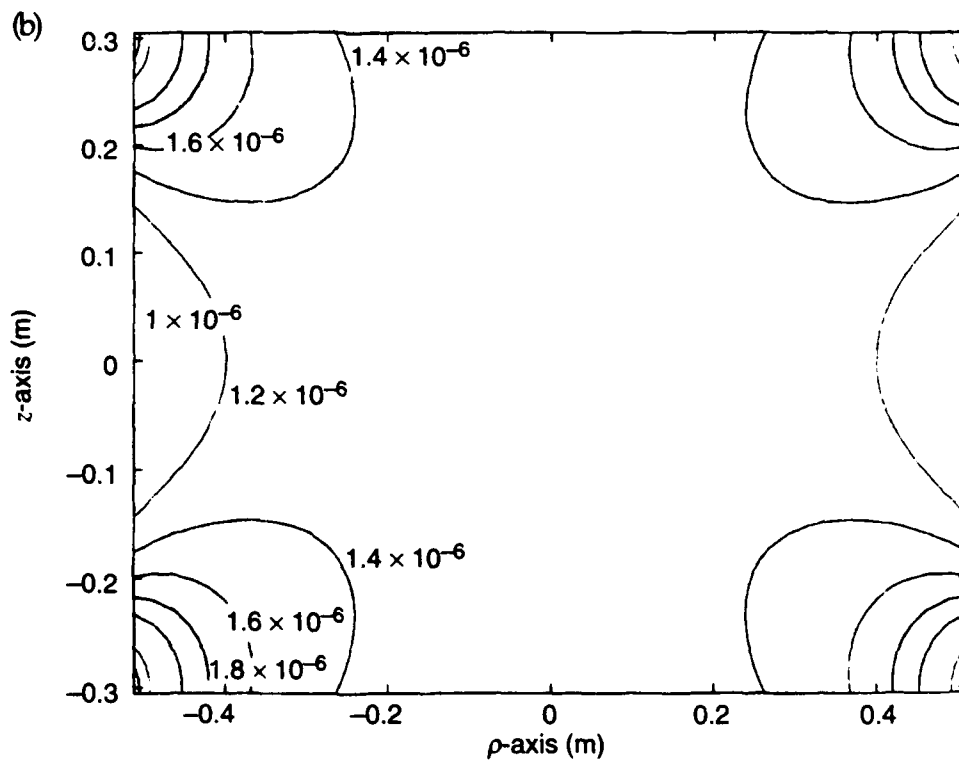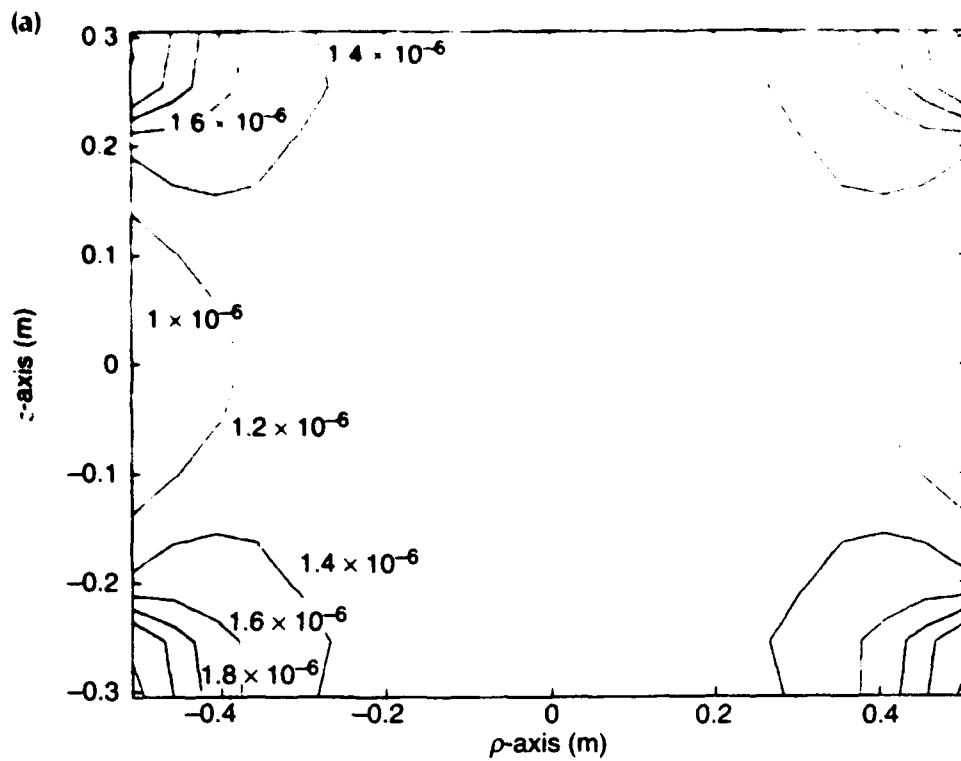
(a)

B(z) magnitude (μT) vs *z*-axis (m)

(b)

B(z) magnitude (μT) vs *z*-axis (m)

Figure 9. Contour plots of *B(z)* **versus** *z* **and** *ρ*: (a) measured and (b) calculated.

(a)

(b)

7. Conclusions

The objective of this report is to provide a technical guideline for the use of the Helmholtz coil that was designed and built for the ARL electromagnetic composite testing laboratory. The experimental versus theoretical results were compared for the primary field component and proved to show excellent correlation. By measuring the current being applied to the coils and using the equations in section 5, the user can predict the magnetic field at any point inside the coils. To assist the user in determining the magnetic fields, we have included appendix A, which is a Matlab® program listing that can be used to generate the graphs as seen in section 6.

The size of the test volume is also an important consideration when working with a Helmholtz coil. The ANSI/ASTM A standard indicates that the test volume is related to the coil diameter. The standard states, "The Helmholtz coil diameter shall be at least three times the length of the test specimen or four times its diameter, or both."[3] Figure 9 confirms this test volume, in that the field is uniform to just over ±0.21 m on the centerline of the ρ-axis (0.34 percent of the diameter) for all values of z. However, figure 9 also shows that the test volume depends on the geometry of the test object. For objects that are less than 0.28 m high (z-axis) and on the centerline, the test area extends to ±0.4 m (ρ-axis). Objects that are more than 0.28 m high have a test area of ±0.21 m (ρ-axis). As a rule of thumb, the coil diameter should be at least three times the length of the test specimen. The test area can be expanded out to about ±0.35 m (ρ-axis) on centerline for all values of z, if a 2-dB change in field uniformity can be tolerated at the corners of the test volume. The reader is referred elsewhere[4] for a complete discussion of how one can extend test volume beyond the above limits for the testing of large objects.

The loading of the coils by the test object has not been addressed in this paper. The user must be aware that a large object of magnetic material placed inside the coil will load the coil and concentrate the fields on the test object. The resultant field will be distorted when compared to the field when the coil was empty. It is recommended that the user measure the current in the empty coil and verify that it does not change when the test object is inserted. If the current does change, the amplifier must be adjusted to the original level.

---

[3]ANSI/ASTM A698-74, American National Standard, Standard Test Method for Magnetic Shield Efficiency in Attenuating Alternating Magnetic Fields (1974).
[4]E. L. Bronaugh, Helmholtz Coils for EMI Immunity Testing: Stretching the Uniform Field Area, Seventh International Conference on Electromagnetic Compatibility (Conf. Publ. No. 326).

17

Appendix A. Matlab Program Listing for Field Calculations

The following is a Matlab program used to calculate the fields at any point inside a Helmholtz coil of Radius *a* and current *I*.

```
% Like loops.m but symmetric plane through z axis
% Computes the B field from 2 thin loops of radius a,
% located at z = +d and -d, (d=a/2, Helmholtz Coils), and
% current I.

LN = 48            % Number of turns in the loops
muo = 4*pi*1e-7;
I=.019052;
a=.6096;
d=a/2;
          % Define the plane over which fields are computed
          % N must be odd to include the point (0,0)
M=26;   % No. of points along the rho axis
N=51;   % No. of points along the z axis
P1=linspace(0,a,M);       % rho always positive
P = [ P1(M:-1:2) P1 ];
Z=linspace(-d,d,N);
[p,z] = meshgrid(P1,Z);   % rho=0, p(:,1); z= -d, z(1,:)


          % Determine modulus and Elliptic Integrals
k1=(4*a*p)./( (a+p).^2 + (z-d).^2 );
[K1,E1] = ellipke(k1);
k2=(4*a*p)./( (a+p).^2 + (z+d).^2 );
[K2,E2] = ellipke(k2);


          % Compute B-rho fields
bp1 = ((z-d)./(p.*sqrt( (a+p).^2 + (z-d).^2 ))) .* ...
( ( (a^2 + p.^2 + (z-d).^2)./((a-p).^2 + (z-d).^2 ) ).*E1 - K1 );
bp2 = ((z+d)./(p.*sqrt( (a+p).^2 + (z+d).^2 ))) .* ...
( ( (a^2 + p.^2 + (z+d).^2)./((a-p).^2 + (z+d).^2 ) ).*E2 - K2 );
bp = ( (LN*muo*I)/(2*pi) )*(bp1 + bp2);
bp(1:N) = zeros(N,1);         % Remove NaN's from rho=0 axis
bp = [ bp(:,M:-1:2) bp ];     % Make it symmetric


          % Compute B-z fields
bz1 = ( 1 ./sqrt( (a+p).^2 + (z-d).^2 ) ) .* ...
( ( (a^2 - p.^2 - (z-d).^2)./((a-p).^2 + (z-d).^2 ) ).*E1 + K1 );
bz2 = ( 1 ./sqrt( (a+p).^2 + (z+d).^2 ) ) .* ...
( ( (a^2 - p.^2 - (z+d).^2)./((a-p).^2 + (z+d).^2 ) ).*E2 + K2 );
bz =   ( (LN*muo*I)/(2*pi) )*(bz1 + bz2);
bz = [ bz(:,M:-1:2) bz ];     % Make it symmetric


          % Compute the total B field
bt = sqrt(bp.^2 + bz.^2);


          % test along the z axis where we know the solution
bzz= 1 ./(sqrt(a^2 + (Z-d).^2)).^3 + 1 ./(sqrt(a^2 + (Z+d).^2)).^3;
bzz = 0.5*LN*muo*I*a^2*bzz;
```

19

Distribution

Admnstr
Defns Techl Info Ctr
Attn DTIC-DDA (2 copies)
Cameron Sta Bldg 5
Alexandria VA 22304-6145

Director
Defns Intllgnc Agcy
Attn DIO/SPRD   D Spohn
Attn RTS-2A Techl Lib
Washington DC 20301

Defns Nuc Agcy
Attn RAAE Atmospheric Effects Div
  B Prasad
Attn RAEE Elect Effects Div
Attn RAEV Electromagnetic Applctn Div
Attn TISI-Scntfc Info Div
6801 Telegraph Rd
Alexandria VA 22310-3398

U.S. Army White Sands Missile Range
Attn STEWS-NE   J Meason
Attn Techl Lib
White Sands Missile Range NM 88002-5030

Dpty Dir for Rsrch & Engrg (Sci & Techlgy)
Attn Rm 3E118, COL J Butt
Pentagon
Washington DC 20301-3080

Ofc of the Assist Scy of the Army for Rsrch
  Dev & Acqstn
Attn SARD-TT   F Milton
Attn SARD-TT   C Nash
Rm 3E479 The Pentagon
Washington DC 20310-0103

Commander
U.S. Army Nuc & Chem Agcy
Attn MONA-NU   A Renner
Attn MONA-NU   R Pfeffer
7150 Heller Loop Rd Ste 101
Springfield VA 22150-3198

US Army Matl Cmnd
Attn AMCAM-CN
5001 Eisenhower Ave
Alexandria VA 22333-0001

Director
US Army Mis Cmnd (USAMICOM)
Attn AMSMI-RD-CS-R Documents
Redstone Arsenal AL 35898-5400

Director
US Army TMDE Actvty
Attn AMXTM-S-A   C Bosco
Redstone Arsenal AL 35898-5400

US Army Rsrch Laboratory
Attn AMSRL-SL-ND   S Share
Aberdeen Proving Ground, MD 21010-5423

Nav Rsrch Lab
Attn 4200 Ctr for Sp Sensing
Attn 4600 Condensed Matter & Radiation Sci
Attn 4700 Plasma Physics Div
Attn 5700 Tactical Elect Warfare Div
Attn 6800 Elect Sci & Techlgy Div
Attn 8000 Ctr for Sp Techlgy
Attn Code 4820 Techl Info Div
4555 Overlook Ave SW
Washington DC 20375-5000

Commander
Nav Surfc Weapons Ctr
Attn Code E231 Techl Lib
Dahlgren VA 22448-5020

US Air Force Phillips Lab
Attn PL/WSR   C Baum
3550 Aberdeen Ave SE
Albuquerque NM 87116-008

HQ USAFA/DFSELD
Attn HQUSAFA/DFSELD
2354 Fairchild Dr Ste 3A22
USAF Academy CO 80840-6214

Distribution

Lawrence Livermore Natl Lab
Attn L-156 M Bland
Attn L-86 H S Cabayan
PO Box 808
Livermore CA 94550

Sandia Natl Lab
Attn Orgn 3141 Reports Acqstn
PO Box 5800
Albuquerque NM 87185

Natl Inst of Stand & Techlgy
Attn V Ulbrecht Rsrch Info Ctr
Rm E01 Bldg 101
Gaithersburg MD 20899

Mssn Rsrch Corp
Attn J Dando
Attn W Stark
4935 N 30th Stret
Colorado Springs CO 80919-3156

US Army Rsrch Lab
Attn AMSRL-OP-SD-TA Mail & Records
  Mgmt
Attn AMSRL-OP-SD-TL Tech Library
  (3 copies)

US Army Rsrch Lab (cont'd)
Attn AMSRL-OP-SD-TP Tech Pub
Attn AMSRL-SL-NB S C Sanders
Attn AMSRL-SS-F Chf
Attn AMSRL-SS-F Dir
Attn AMSRL-SS-S Chf
Attn AMSRL-SS-S Dir
Attn AMSRL-WT-N Senior Research Scientist
Attn AMSRL-WT-NB Chf
Attn AMSRL-WT-ND D DeTroye
  (10 copies)
Attn AMSRL-WT-ND R J Chase
  (10 copies)
Attn AMSRL-WT-ND R L Atkinson
Attn AMSRL-WT-NF R Kaul
Attn AMSRL-WT-NG Chf
Attn AMSRL-WT-NI Chf
Attn AMSRL-WT-NW Deputy Director
Attn AMSRL-WT-P Chf
Attn AMSRL-WT-T Chf
Attn AMSRL-WT-W Chf